ACS APPLIED MATERIALS & INTERFACES

Research Article

www.acsami.org

High-Surface-Area Architectures for Improved Charge Transfer Kinetics at the Dark Electrode in Dye-Sensitized Solar Cells

William L. Hoffeditz,[†,‡] Michael J. Katz,[†] Pravas Deria,[†] Alex B.F. Martinson,[‡,§] Michael J. Pellin,[†,‡,§] Omar K. Farha,*[,†,∥] and Joseph T. Hupp*[,†,‡,§,#]

[†]Department of Chemistry, Northwestern University, 2145 Sheridan Road, Evanston, Illinois 60208, United States

[‡]Argonne-Northwestern Solar Energy Research (ANSER) Center, [§]Material Science Division, and [#]Chemical Sciences and Engineering Division, Argonne National Laboratory, 9700 South Cass Avenue, Argonne, Illinois 60439, United States

[∥]Department of Chemistry, Faculty of Science, King Abdulaziz University, Jeddah, Saudi Arabia

Supporting Information

ABSTRACT: Dye-sensitized solar cell (DSC) redox shuttles other than triiodide/iodide have exhibited significantly higher charge transfer resistances at the dark electrode. This often results in poor fill factor, a severe detriment to device performance. Rather than moving to dark electrodes of untested materials that may have higher catalytic activity for specific shuttles, the surface area of platinum dark electrodes could be increased, improving the catalytic activity by simply presenting more catalyst to the shuttle solution. A new copper-based redox shuttle that experiences extremely high charge-transfer resistance at conventional Pt dark electrodes yields cells having fill-factors of less than 0.3. By replacing the standard Pt dark electrode with an inverse opal Pt electrode fabricated via atomic layer deposition, the dark electrode surface area is boosted by ca. 50-fold. The resulting increase in interfacial electron transfer rate (decrease in charge-transfer resistance) nearly doubles the fill factor and therefore the overall energy conversion efficiency, illustrating the utility of this high-area electrode for DSCs

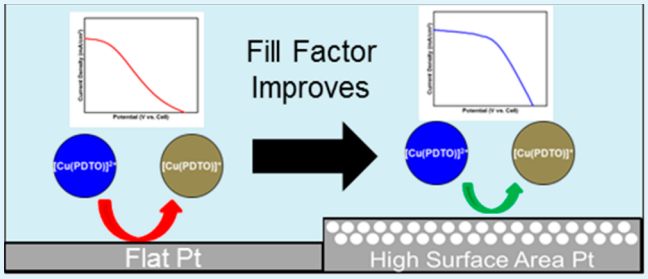

KEYWORDS: *dark electrode, inverse opal, dye cell, fill factor*

INTRODUCTION

Dye-sensitized solar cells (DSCs) are an oft-studied alternative to traditional Si-based photovoltaic technology.[1−4] Broadly popularized by O'Regan and Graetzel in 1991, DSCs featuring nanoparticulate photoanodes of TiO_2 were quickly pushed to power conversion efficiencies above 10%.[5,6] The most common optimized devices incorporate triiodide/iodide (I_3^-/I^-) as the electron shuttle.[4] The greatest single opportunity for efficiency improvement would appear to be in increasing open-circuit voltages by largely eliminating the sizable driving force needed for dye regeneration by iodide.[7] Recent attempts at solving this problem have tended to focus on moving away from I_3^-/I^-, and instead deploying various cobalt,[8−10] copper,[11,12] iron,[13,14] or nickel-based[15] outer-sphere redox couples in addition to organic molecule shuttles[16] and solid-state hole conductors.[17] Each of these innovations has aimed at increasing the overall power conversion efficiency (η) of DSCs, but the innovations themselves focus almost entirely on the photoelectrode. However, improvements at the dark electrode can also lead to improved power conversion efficiencies. Thus, we demonstrate how increasing the surface area of a platinum dark electrode can nearly double the efficiency of a particularly challenging cell that utilizes a new system, 1,8-bis(2′-pyridyl)-3,6-dithiaoctane copper(II)/(I) ($Cu(PDTO)^{2+/+}$), as the redox shuttle;[18] see Figure 1.

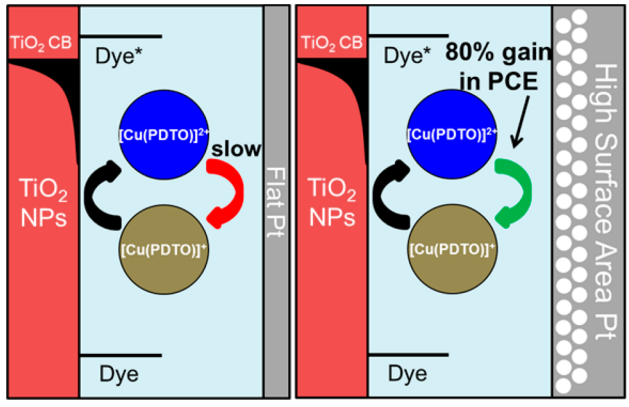

Figure 1. Basic components of a DSC highlighting the location of the major loss in efficiency due to the dark electrode of the device discussed.

The benefits of improving performance at the dark electrode are most clearly seen in the improvement of the oft-neglected fill-factor variable and its subsequent effect on η. Power

Received: March 12, 2014
Accepted: May 5, 2014
Published: May 14, 2014

conversion efficiency is calculated as in eq 1, where J_{sc}, V_{oc}, and P_{in} represent short circuit current, open circuit voltage and incident power, respectively. FF represents the fill factor, which is related to the maximum power point of a device. A poor fill factor is typically the result of undesirable resistances within the device. This term is often taken for granted in traditionally constructed devices (i.e., those utilizing I_3^-/I^- and a ruthenium-based dye) because its value is reasonably close to optimal. However, as new shuttles have been employed, focusing on this this term has become more important. Previous work has shown that Co(2,2′-bipyridine)$_3^{3+/2+}$, perhaps the most successful alternative shuttle, displays more favorable electrochemistry (faster charge-transfer kinetics) on electrodes other than platinum, i.e., gold, carbon, or polymer electrodes, among others;[19,20] when traditional platinum electrodes are used, the fill factor, and thus the efficiency, suffers.[21]

$$\eta = \frac{J_{sc} V_{oc} FF}{P_{in}} \quad (1)$$

While a specific shuttle may benefit greatly from a novel counter electrode, the new counter electrode may not be advantageous with all potential shuttles and, with some shuttles, may actually lead to a decrease in performance.[22,23] For example, when an inverse opal (IO) architecture was utilized with carbon-based dark electrodes, performance with the I_3^-/I^- shuttle was worse than with traditional platinum dark electrodes.[24] Additionally, some alternative dark electrodes may be difficult to fabricate, introducing complications in the scaling and/or commercialization of DSCs. Ideally, an improved dark electrode could be applied to and work well for nearly all possible redox shuttle systems. Instead of devising a dark electrode that can yield larger rate constants than can traditional Pt dark electrodes for electron transfer to a given redox shuttle, we choose here to increase the surface area of the Pt dark electrode. Thus, in terms of effects on electron-transfer rate, a 10-fold increase in electrode surface area would be equivalent to a 10-fold increase in heterogeneous electrochemical rate constant. To this end, we use a new redox shuttle to illustrate that large charge-transfer resistances for its reaction at the dark electrode lead to a large decrease in overall cell efficiency. We then rectify this problem by shifting to a high-area platinum dark electrode fabricated on an IO architecture by using atomic layer deposition (ALD).[25]

EXPERIMENTAL SECTION

Unless otherwise noted, all chemicals were purchased from Sigma-Aldrich and used as received. Fluorine-doped tin oxide (FTO) glass was purchased from Hartford Glass (Hartford City, IN). Polystyrene microspheres (average diameter 350 nm) were purchased from Alfa-Aesar. TiO_2 nanoparticles were purchased from Dyesol. The platinum ALD precursor (trimethyl)methylcyclopentadienylplatinum(IV) was purchased from Strem. The 1,8-bis(2′-pyridyl)-3,6-dithiaoctane (PDTO) ligand was synthesized by the method of Goodwin and Lions[26] and recrystallized from hot hexanes. [Cu(PDTO)](CF$_3$SO$_3$)$_2$ (Figure 2) was formed by mixing in ∼1:1 ratio by mol copper(II) triflate with PDTO in acetonitrile and rotovapping to dryness. [Cu(PDTO)](CF$_3$SO$_3$)$_1$ was generated in situ by addition of dendritic copper powder to a 1:1 mixture of [Cu(PDTO)](CF$_3$SO$_3$)$_2$:PDTO in acetonitrile. [Co(2,2′-bipyridine)$_3$](PF$_6$) (Co(bpy)$_3^{3+/2+}$) salts were synthesized by mixing Co(NO$_3$)$_2$ with 2,2′-bipyridine in a 1:3.1 ratio in methanol followed by the addition of an excess of NH_4PF_6. A portion of the resulting [Co(bpy)$_3$]$^{2+}$ was oxidized to [Co(bpy)$_3$]$^{3+}$ by the addition of $NOBF_4$ and precipitated by addition of water. The

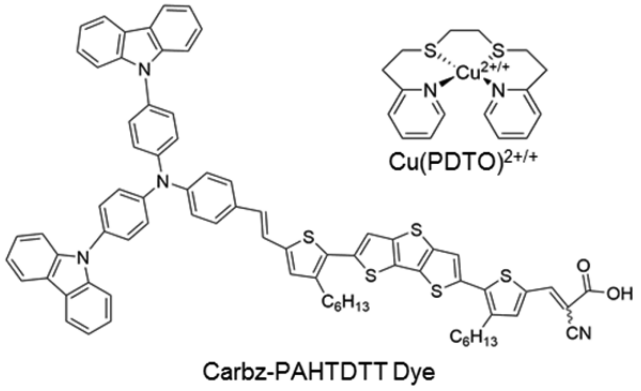

Figure 2. Carbz-PAHTDTT dye and Cu(PDTO)$^{2+/+}$ redox shuttle.

Carbz-PAHTDTT dye (Figure 2) was synthesized according to literature procedure.[13]

FTO glass cut in 2 cm × 2 cm squares with a machined hole for electrolyte solution loading was the basis for all counter electrodes in two electrode experiments. All glass was cleaned by sonication in detergent, isopropanol, and methanol before use. IOs were grown by the method of Hatton, et al.[27] and then platinized via ALD in a Savannah 200 reactor manufactured by Ultratech/Cambridge Nano-Tech. The Pt precursor was held at 75 °C, and 500 alternating cycles of Pt (1 s pulse, 5 s expo, 8 s nitrogen purge) and O_2 (2 s pulse, 9 s nitrogen purge) resulted in ∼12 nm of Pt growth on the IO framework. Platinum thermal decomposition counter electrodes (TD Pt) were formed by drop casting a H_2PtCl_6 solution on FTO glass and heating at 500 °C for 20 min. For two-electrode impedance measurements, two IO or TD Pt electrodes were sandwiched using a Surlyn spacer with a 0.25 cm^2 hole to define the active area of the counter electrode, as shown in Figure 3. Dye-cell photoanodes

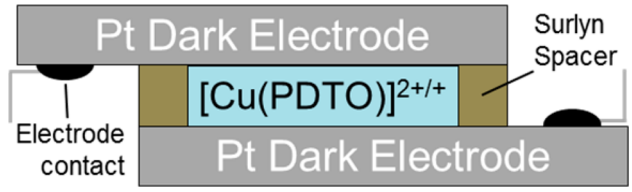

Figure 3. Schematic representation of the two-electrode set-up used in all impedance measurements.

(nanoparticulate TiO_2 on FTO, 6 micrometers thick; no scattering layer[28]) were prepared by standard methods and dye loaded overnight in Carbz-PAHTDTT dye (0.2 mM) in 3:2 chloroform:ethanol solution containing 20 mM chenodeoxycholic acid (to inhibit aggregation of the adsorbed form of the dye). Photoanodes were sandwiched and heat-sealed (using a Surlyn spacer) with either IO Pt or TD Pt counter electrodes and vacuum back-loaded with the desired electrolyte solution. Photoanodes for three-electrode experiments were prepared in the same manner without sandwiching.

All redox solutions were made in acetonitrile. I_3^-/I^- solutions contained 0.6 M 1,2-dimethyl-3-propylimidazolium iodide, 0.05 M I_2, and 0.5 M 4-*tert*-butylpyridine (tbp). Co(bpy)$_3^{3+/2+}$ solutions consisted of 0.2 M [Co(bpy)$_3$](PF$_6$)$_2$, 0.02 M [Co(bpy)$_3$](PF$_6$)$_3$, and 0.5 M tbp. Cu(PDTO)$^{2+/+}$ solutions were 0.5 M [Cu(PDTO)](CF$_3$SO$_3$), 0.05 M [Cu(PDTO)](CF$_3$SO$_3$)$_2$, and 0.5 tbp.

Electrochemical impedance measurements were taken on a Solartron 1286 electrochemical interface coupled to a SI 1260 impedance/gain-phase analyzer using the two-dark-electrode setup depicted in Figure 3 with shuttle concentrations identical to those used in constructed photocells. Photo-electrochemical measurements were performed using a Jobin-Yvon Fluorolog-3 fluorimeter with a xenon-arc lamp and AM-1.5 filter as the light source and a Solartron Analytical Modulab potentiostat. Three-electrode measurements were

performed with a platinum mesh counter electrode and KCl saturated Ag/AgCl reference electrode in 1 mL of $Cu(PDTO)^{2+/+}$-containing solution using dye-loaded TiO_2 as the working electrode.

RESULTS AND DISCUSSION

Electrochemical impedance spectroscopy was used to determine magnitudes of charge resistance at TD Pt electrodes, first with the common I_3^-/I^- and $Co(bpy)_3^{3+/2+}$ redox shuttles and then with the new copper-based shuttle, using the experimental setup shown in Figure 3. The resulting Nyquist plots for no applied bias are shown in Figure 4 (red, green, and brown

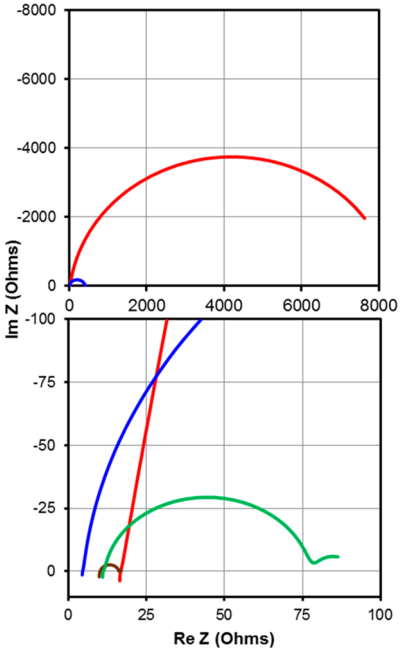

Figure 4. Nyquist plots at high resistances (top) and zoomed in to low resistances (bottom) for two-electrode impedance measurements utilizing TD Pt dark electrodes and I_3^-/I^- (brown), $Co(bpy)_3^{3+/2+}$ (green), and $Cu(PDTO)^{2+/+}$ (red) redox shuttle solutions and for an IO Pt dark electrode (blue) with $Cu(PDTO)^{2+/+}$.

lines). The Nyquist plots were fit to the equivalent circuit in Figure S1 in the Supporting Information. For all three redox shuttles, the Nyquist plot contained one primary arc. This arc is attributed to the charge transfer resistance (R_{CT}) at the electrode. (Recall that R_{CT} scales inversely with the rate of interfacial (electrochemical) electron transfer.) A second arc for I_3^-/I^- and $Co(bpy)_3^{3+/2+}$ is observed at high resistance; this is due to the solution diffusion, which is fit to a Warburg element.[29] In the case of $Cu(PDTO)^{2+/+}$ with TD Pt, the diffusion element cannot be easily identified due to the exceptionally large charge-transfer resistance. Using an asymmetric setup of Figure 3 (i.e., one IO Pt electrode as the "working electrode" and one TD Pt electrode) with $Cu(PDTO)^{2+/+}$ results in the blue Nyquist plot in Figure 4.

Fits of the Nyquist plots in Figure 4 to the circuit in Figure S1 in the Supporting Information demonstrated errors of less than 10% and showed the charge transfer resistance of the $Cu(PDTO)^{2+/+}$ system (4400 ohms) with TD Pt to be ~1000x higher than that of I_3^-/I^- (1.5 ohms) and ~100× higher than that of $Co(bpy)_3^{3+/2+}$ (65 ohms). The charge transfer resistance at the dark electrode is inversely proportional to the rate of charge transfer; therefore, as the R_{CT} for $Cu(PDTO)^{2+/+}$ is ~1000× larger than I_3^-/I^-, we can estimate the rate of charge transfer to also be ~1000× slower (~70× slower than $Co(bpy)_3^{3+/2+}$). DSCs utilizing $Co(bpy)_3^{3+/2+}$ shuttle and TD Pt counter electrodes have shown diminished fill factor at full illumination,[21] suggesting that the $Cu(PDTO)^{2+/+}$ shuttle in an identical system will suffer from the same problem much more seriously.

Clearly, because of the high charge transfer resistance of the $Cu(PDTO)^{2+/+}$ on TD Pt, a different approach was required. To this end, high area IO Pt counter electrodes were employed. Utilization of an IO Pt dark electrode in one half of the setup shown in Figure 3 resulted in a charge transfer resistance of 400 ohms, 10× less than that of devices using all TD Pt electrodes. IO Pt offers increased counter electrode activity (via increased surface area) without the added complications of general material applicability as discussed above. Also, because of the large apertures in this IO framework, diffusional constraints that often hamper high area architectures will not be present.[30] Cyclic voltammograms (CV) of the IO Pt frameworks compared to CVs of flat ALD Pt electrodes in 2 molar H_2SO_4 (see Figure S2 in the Supporting Information) reveal a surface area increase of ~50. The deposited thickness of Pt is approximately 12 nm (by in situ quartz crystal microbalance), meaning that only ~5 mg of Pt is required to fully coat a 2 cm × 2 cm IO with this surface area enhancement.

DSCs were fabricated using both TD Pt and IO Pt as counter electrodes with $Cu(PDTO)^{2+/+}$ as the redox shuttle. Photoelectrochemical measurements were performed, and the resulting current-voltage curves are shown in Figure 5. The

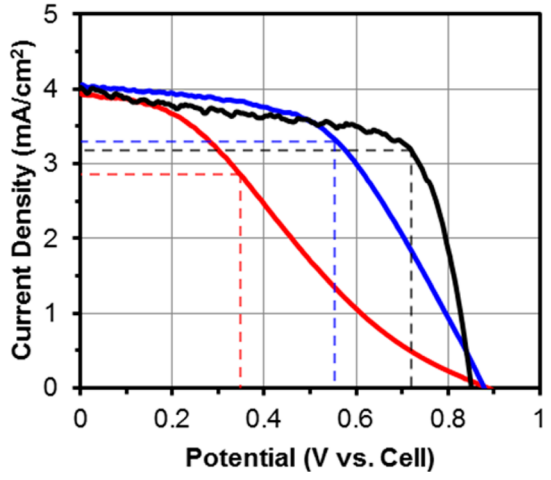

Figure 5. Current−potential curves for DSCs utilizing $Cu(PDTO)^{2+/+}$ redox shuttle and TD Pt dark electrode (red), IO Pt dark electrode (blue), and in a three-electrode (as opposed to two electrode) set up (black). Dashed lines represent the maximum power points of the individual JV curves.

J_{sc} and V_{oc} of these devices are essentially identical when accounting for normal variations between devices. This is expected for V_{oc} as the dark electrode resistance will not be a factor when current is zero, meaning no correction for resistance is necessary. In principle, lowering the charge resistance at the dark electrode can also influence J_{sc}.[31] However, as charge transfer at the dark electrode is not the primary current limiter in this system when the photovoltage is zero, no improvement in J_{sc} is seen when switching to the IO Pt dark electrode. The current does improve at potentials between

zero and V_{oc} since when both current and voltage have non-zero values, the resistance at the dark electrode becomes a factor. This affects the FF of the device and results in the curve shape seen for the TD Pt dark electrode in Figure 5 (red). Because IO Pt dark electrodes lower the resistance of the dark electrode via increased surface area, there is clear improvement in fill factor. This increase in fill factor (FF = 0.28 for TD Pt, 0.52 for IO Pt) leads to an 80% increase in power conversion efficiency from 1 to 1.8%. This dramatic improvement is attributed to the IO Pt possessing ∼50 times higher surface area than than does TD Pt, resulting in IO Pt performing as if it is a 50× faster catalyst for turning over the $Cu(PDTO)^{2+/+}$ redox shuttle.

A three-electrode measurement (black curve) was performed to determine the hypothetical best case scenario in terms of improving the fill factor of the system. In the presence of a reference electrode, the counter electrode can be held at any potential necessary to ensure the working electrode is at the desired potential.[32] Therefore, any current flow limitations due to the performance of the dark electrode in a two-electrode system (such as a DSC) will be absent, providing a comparison point for the improvement seen with IO Pt vs. TD Pt dark electrodes in two-electrode systems. (It should be noted that the three-electrode measurement was performed under higher light intensity to obtain comparable short-circuit currents as a large diffusion resistance due to the distances in the experimental set up. The potential scale was also adjusted from Ag/AgCl to that of the redox shuttle used in two-electrode measurements by adjusting to the Nernstian potential of the electrolyte solution vs. Ag/AgCl). The three-electrode results show that room remains for improvement in the fill factor based on improved dark electrode performance. The simplest way to achieve this would be through further increase in the surface area of the dark electrode.

CONCLUSIONS

By using a redox shuttle having larger charge-transfer resistances at TD Pt electrodes (dark electrodes) than common shuttles such as I_3^-/I^- and $Co(bpy)_3^{3+/2+}$, the consequences of kinetically limited shuttle behavior upon DSC fill factors and overall energy conversion efficiencies can be readily observed. A new approach to addressing this problem (i.e. slow dark-electrode kinetics and concomitant fill-factor degradation) was examined. To decrease charge-transfer resistances (increase charge-transfer rates) at the dark electrode, high area IO platinum electrodes were fabricated utilizing platinum ALD. When used in conjunction with $Cu(PDTO)^{2+/+}$ as the shuttle in otherwise conventional DSCs, the IO Pt electrodes nearly doubled the fill factor, and therefore, nearly doubled the efficiency as well. Because our design principle focuses on increasing the electron-transfer rate, rather than the rate constant, the need to discover dark electrode catalysts for "problematic" shuttles is diminished. However, because this approach is rate constant independent, it may still be applied to other catalytic materials with improved rate constants for electron-transfer but lower than ideal fill-factors with "problematic" shuttles. Thus, applying our approach to a specific catalyst-shuttle system can lead to improved efficiency across many varying systems.

ASSOCIATED CONTENT

Supporting Information

Equivalent circuit and CVs for surface area determination. This material is available free of charge via the Internet at http://pubs.acs.org.

AUTHOR INFORMATION

Corresponding Authors

*E-mail: j-hupp@northwestern.edu.
*E-mail: o-farha@northwestern.edu.

Notes

The authors declare no competing financial interest.

ACKNOWLEDGMENTS

This work was supported as part of the ANSER Center, an Energy Frontier Research Center funded by the U.S. Department of Energy, Office of Science, Office of Basic Energy Sciences, under Award DE-SC0001059.

REFERENCES

(1) Hardin, B. E.; Snaith, H. J.; McGehee, M. D. The Renaissance of Dye-Sensitized Solar Cells. *Nat. Photonics* **2012**, *6*, 162−169.
(2) Labat, F.; Le Bahers, T.; Ciofini, I.; Adamo, C. First-Principles Modeling of Dye-Sensitized Solar Cells: Challenges and Perspectives. *Acc. Chem. Res.* **2012**, *45*, 1268−1277.
(3) Cong, J.; Yang, X.; Kloo, L.; Sun, L. Iodine/Iodide-Free Redox Shuttles for Liquid Electrolyte-Based Dye-Sensitized Solar Cells. *Energy Environ. Sci.* **2012**, *5*, 9180−9194.
(4) Hagfeldt, A.; Boschloo, G.; Sun, L.; Kloo, L.; Pettersson, H. Dye-Sensitized Solar Cells. *Chem. Rev.* **2010**, *110*, 6595−6663.
(5) O'Regan, B.; Gratzel, M. A Low-Cost, High-Efficiency Solar Cell Based on Dye-Sensitized Colloidal Tio2 Films. *Nature* **1991**, *353*, 737−740.
(6) Nazeeruddin, M. K.; Kay, A.; Rodicio, I.; Humphry-Baker, R.; Mueller, E.; Liska, P.; Vlachopoulos, N.; Graetzel, M. Conversion of Light to Electricity by Cis-X2bis(2,2′-Bipyridyl-4,4′-Dicarboxylate)-Ruthenium(II) Charge-Transfer Sensitizers (X = Cl-, Br-, I-, CN-, and SCN-) on Nanocrystalline Titanium Dioxide Electrodes. *J. Am. Chem. Soc.* **1993**, *115*, 6382−6390.
(7) Snaith, H. J. Estimating the Maximum Attainable Efficiency in Dye-Sensitized Solar Cells. *Adv. Funct. Mater.* **2010**, *20*, 13−19.
(8) Yella, A.; Lee, H.-W.; Tsao, H. N.; Yi, C.; Chandiran, A. K.; Nazeeruddin, M. K.; Diau, E. W.-G.; Yeh, C.-Y.; Zakeeruddin, S. M.; Grätzel, M. Porphyrin-Sensitized Solar Cells with Cobalt (II/III)−Based Redox Electrolyte Exceed 12 Percent Efficiency. *Science* **2011**, *334*, 629−634.
(9) Feldt, S. M.; Gibson, E. A.; Gabrielsson, E.; Sun, L.; Boschloo, G.; Hagfeldt, A. Design of Organic Dyes and Cobalt Polypyridine Redox Mediators for High-Efficiency Dye-Sensitized Solar Cells. *J. Am. Chem. Soc.* **2010**, *132*, 16714−16724.
(10) Hamann, T. W. The End of Iodide? Cobalt Complex Redox Shuttles in Dsscs. *Dalton Trans.* **2012**, *41*, 3111−3115.
(11) Bai, Y.; Yu, Q.; Cai, N.; Wang, Y.; Zhang, M.; Wang, P. High-Efficiency Organic Dye-Sensitized Mesoscopic Solar Cells with a Copper Redox Shuttle. *Chem. Commun.* **2011**, *47*, 4376−4378.
(12) Hattori, S.; Wada, Y.; Yanagida, S.; Fukuzumi, S. Blue Copper Model Complexes with Distored Tetragonal Geometry Acting as Effective Electron-Transfer Mediators in Dye-Sensitized Solar Cells. *J. Am. Chem. Soc.* **2005**, *127*, 9648−9654.
(13) Daeneke, T.; Kwon, T. H.; Holmes, A. B.; Duffy, N. W.; Bach, U.; Spiccia, L. High-Efficiency Dye-Sensitized Solar Cells with Ferrocene-Based Electrolytes. *Nat. Chem.* **2011**, *3*, 211−215.
(14) Hamann, T. W.; Farha, O. K.; Hupp, J. T. Outer-Sphere Redox Couples as Shuttles in Dye-Sensitized Solar Cells. Performance Enhancement Based on Photoelectrode Modification Via Atomic Layer Deposition. *J. Phys. Chem. C* **2009**, *112*, 19756−19764.

(15) Li, T. C.; Spokoyny, A. M.; She, C.; Farha, O. K.; Mirkin, C. A.; Marks, T. J.; Hupp, J. T. Ni(III)/(IV) Bis(Dicarbollide) as a Fast, Noncorrosive Redox Shuttle for Dye-Sensitized Solar Cells. *J. Am. Chem. Soc.* **2012**, *132*, 4580−4582.
(16) Wang, M.; Chamberland, N.; Breau, L.; Moser, J.-E.; Humphry-Baker, R.; Marsan, B.; Zakeeruddin, S. M.; Graetzel, M. An Organic Redox Electrolyte to Rival Triiodide/Iodide in Dye-Sensitized Solar Cells. *Nat. Chem.* **2010**, *2*, 385.
(17) Burschka, J.; Dualeh, A.; Kessler, F.; Baranoff, E.; Cevey-Ha, N. L.; Yi, C.; Nazeeruddin, M. K.; Gratzel, M. Tris(2-(1h-Pyrazol-1-Yl)Pyridine)Cobalt(III) as P-Type Dopant for Organic Semiconductors and Its Application in Highly Efficient Solid-State Dye-Sensitized Solar Cells. *J. Am. Chem. Soc.* **2011**, *133*, 18042−18045.
(18) A full report on the behavior of the new shuttle in various DSCs will be presented elsewhere.
(19) Sapp, S. A.; Elliott, C. M.; Contado, C.; Caramori, S.; Bignozzi, C. A. Substituted Polypyridine Complexes of Cobalt(II/III) as Efficient Electron-Transfer Mediators in Dye-Sensitized Solar Cells. *J. Am. Chem. Soc.* **2002**, *124*, 11215−11222.
(20) Yum, J.-H.; Baranoff, E.; Kessler, F.; Moehl, T.; Ahmad, S.; Bessho, T.; Marchioro, A.; Ghadiri, E.; Moser, J.-E.; Yi, C.; Nazeeruddin, M. K.; Grätzel, M. A Cobalt Complex Redox Shuttle for Dye-Sensitized Solar Cells with High Open-Circuit Potentials. *Nat. Commun.* **2012**, *3*, 631.
(21) Stefik, M.; Yum, J.-H.; Hu, Y.; Gratzel, M. Carbon-Graphene Nanocomposite Cathodes for Improved Co(II/III) Mediated Dye-Sensitized Solar Cells. *J. Mater. Chem. A* **2013**, *1*, 4982−4987.
(22) Ku, Z.; Li, X.; Liu, G.; Wang, H.; Rong, Y.; Xu, M.; Liu, L.; Hu, M.; Yang, Y.; Han, H. Transparent NiS Counter Electrodes for Thiolate/Disulfide Mediated Dye-Sensitized Solar Cells. *J. Mater. Chem. A* **2013**, *1*, 237−240.
(23) Jhang, Y.-H.; Tsai, Y.-T.; Tsai, C.-H.; Hsu, S.-Y.; Huang, T.-W.; Lu, C.-Y.; Chen, M.-C.; Chen, Y.-F.; Wu, C.-C. Nanostructured Platinum Counter Electrodes by Self-Assembled Nanospheres for Dye-Sensitized Solar Cells. *Org. Electron.* **2012**, *13*, 1865−1872.
(24) Kang, D.-Y.; Lee, Y.; Cho, C.-Y.; Moon, J. H. Inverse Opal Carbons for Counter Electrode of Dye-Sensitized Solar Cells. *Langmuir* **2012**, *28*, 7033−7038.
(25) Alternative methods of making platinum-coated IOs are known and have been used for methanol oxidation. See Liu, Y.; Chen, J.; Misoska, V.; Swiegers, G. F.; Wallace, G. G. *Mater. Lett.* **2007**, *61*, 2887.
(26) Goodwin, H. A.; Lions, F. Quadridentate Chelate Compounds. II. *J. Am. Chem. Soc.* **1960**, *82*, 5013−5023.
(27) Hatton, B.; Mishchenko, L.; Davis, S.; Sandhage, K. H.; Aizenberg, J. Assembly of Large-Area, Highly Ordered, Crack-Free Inverse Opal Films. *Proc. Natl. Acad. Sci. U.S.A.* **2010**, *107*, 10354−10359.
(28) Since our goal was to understand and examine issues relating to dark-electrode behavior, and not to build champion or near-champion devices, we did not attempt to optimize photoelectrode designs, dye loading, or other factors.
(29) Hauch, A.; Georg, A. Diffusion in the Electrolyte and Charge-Transfer Reaction at the Platinum in Dye-Sensitized Solar Cells. *Electrochim. Acta* **2001**, *46*, 3457−3466.
(30) Klahr, B. M.; Hamann, T. W. Performance Enhancement and Limitations of Cobalt Bipyridyl Redox Shuttles in Dye-Sensitized Solar Cells. *J. Phys. Chem. C* **2009**, *113*, 14040−14045.
(31) Hod, I.; Tachan, Z.; Shalom, M.; Zaban, A. Internal Photoreference Electrode: A Powerful Characterization Method for Photoelectrochemical Quantum Dot Sensitized Solar Cells. *J. Phys. Chem. Lett.* **2011**, *2*, 1032−1037.
(32) Hodes, G. Photoelectrochemical Cell Measurements: Getting the Basics Right. *J. Phys. Chem. Lett.* **2012**, *3*, 1208−1213.